

MODELLING SQUEEZE FLOW OF VISCOUS POLYMER MELTS

TRISTAN J. SHELLEY¹, XIAOLIN LIU², MARTIN VEIDT³, MICHAEL
HEITZMANN⁴ AND ROWAN PATON⁵

¹ School of Mechanical and Mining Engineering
The University of Queensland, 4067, QLD, Australia
and
Cooperative Research Centre for Advanced Composite Structures Ltd (CRC-ACS)
50 Schneider Road, Eagle Farm, 4009, QLD, Australia
e-mail: t.shelley@uq.edu.au, www.mech.uq.edu.au/ultracomp/composites/people/shelley/

² Cooperative Research Centre for Advanced Composite Structures Ltd (CRC-ACS) and
Advanced Composite Structures Australia Pty Ltd (ACS-A)
1/320 Lorimer Street, Port Melbourne, 3207, VIC, Australia
email: x.liu@crc-accs.com.au

³ School of Mechanical and Mining Engineering
The University of Queensland, 4067, QLD, Australia
e-mail: m.veidt@uq.edu.au, www.mech.uq.edu.au/ultracomp/ultrasonics/people/veidt/

⁴ Cooperative Research Centre for Advanced Composite Structures Ltd (CRC-ACS) and
Advanced Composite Structures Australia Pty Ltd (ACS-A)
50 Schneider Road, Eagle Farm, 4009, QLD, Australia
e-mail: m.heizmann@crc-accs.com.au

⁵ Cooperative Research Centre for Advanced Composite Structures Ltd (CRC-ACS) and
Advanced Composite Structures Australia Pty Ltd (ACS-A)
1/320 Lorimer Street, Port Melbourne, 3207, VIC, Australia
e-mail: r.paton@crc-accs.com.au

Key Words: *Squeeze Flow, Finite Element Analysis, Thermoplastics, Welding*

Summary. In the present work, squeeze flow between rigid platens of viscous polymer melts is investigated through two-dimensional finite element simulations using MSC Mentat/MSC Marc. The polymer under investigation is a thermoplastic processed above its melt temperature. The aim of the present work is to develop and validate a finite element modelling framework capable of simulating squeeze flow for a range of geometries and processing parameters. The models will be used to analyse the thickness evolution of the polymer film over time, as well as the shape and volume of the spew fillet; the simulation framework is to be validated using analytical solutions. Initial validations resulted in an average difference of 1% between the analytical and FEA solutions for final thickness of the weld polymer, with a maximum difference of 3.47%. The intention is to extend the

simulations to be capable of representing non-Newtonian viscosities in the fluid model due to variations in the processing temperature.

1 INTRODUCTION

Analyses of squeeze flows (also known as squeeze films or upsetting [1]) have been widely studied for over 100 years, most notably for lubrication applications (e.g. bearings). Squeeze flow is defined as '*a flow in which a material is deformed between two parallel or nearly parallel boundaries approaching each other*' [2]. The first people to develop equations related to squeeze flows were Stefan and Reynolds in the late 19th century [3, 4]. Reynolds developed a series of assumptions and provided the basis for which squeeze flows have been analysed. Analytical solutions for squeeze flow are well developed in literature for both parallel plates [3, 5-7] and non-parallel plates [8, 9].

The use of FEA methods for the analysis of squeeze flow has become more prevalent over the past 10-20 years [1, 10-16]. Research into FEA methods for the analysis of squeeze casting has been identified [17-19]. The analysis of squeeze flow using FEA methods has many advantages over the analytical methods. These include greater details in the flow velocity and pressure distributions and the characterisation of the free surface shape (most notably the spew fillet). FEA methods allow for problems with complicated three-dimensional (3D) geometries or complex viscosity models to be successfully modelled whilst analytical methods are generally restricted to simple two-dimensional (2D) geometry and Newtonian fluids.

In the present work, a rigid-plastic, finite element solver implemented in MSC/Marc was used to model squeeze flow of viscous polymer melts between rigid platens. The intended applications of the modelling are to simulate the flow of weld thermoplastic during a process for welding composite laminates. Two-dimensional finite element analyses were conducted with both Newtonian and non-Newtonian viscosity models. The FEA predictions using the Newtonian model were compared with those obtained by analytical solutions. They were in excellent agreement, indicating that finite element models provide accurate solutions to the squeeze flow problems considered. The finite element framework developed in this study will allow for the analysis of more complicated and practical squeeze flow problems encountered in the welding process, such as problems involving complex geometry and/or non-Newtonian fluids, and flows between elastically deforming composite laminates in the future.

2 ANALYTICAL SQUEEZE FLOW MODELS

In deriving analytical solutions to the squeeze flow of viscous fluids, Reynolds assumed that: (i) gravitational and inertial terms were negligible, (ii) the fluid was Newtonian, isoviscous and incompressible, (iii) thickness of the squeeze film was small compared with the platen dimensions, (iv) there was no slip at the boundaries between the fluid and the platen, and (v) there were no surface tension effects.

Two geometries are commonly considered in the literature: parallel discs (axi-symmetrical flow) [5, 20-26] and infinite length parallel plates for which flow occurs on the plane of cross section (plane-strain flow) [5, 6]. Fuller begins his analysis of squeeze films by analysing bearing lubrication; this analysis leads to a general equation (Equation 1) for any fluid flowing through a slot (Figure 1). This equation forms the basis necessary for solving both the

axi-symmetrical flow and plane-strain flow [5].

$$Q = \frac{\Delta P l h^3}{12 \eta b} \quad (1)$$

Where (see Figure 1):
 Q – volume of flow
 ΔP – pressure difference, from P_1 to P_2
 h – thickness of slot
 b – width of slot
 η – viscosity
 l – length

The derivations to obtain the solutions for parallel discs and infinite length parallel plates are given in Reference [5]. The equations derived are Equation 2 for axi-symmetrical flow and Equation 3 for plane-strain flow respectively.

$$t = \frac{3\pi\eta R^4}{4W} \left[\frac{1}{h_1^2} - \frac{1}{h_0^2} \right] \quad (2)$$

Where:
 t – time
 R – radius of disc
 W – load
 h_1 – thickness of slot
 h_0 – initial thickness of slot

$$t = \frac{l\mu b^3}{2W} \left[\frac{1}{h_1^2} - \frac{1}{h_0^2} \right] \quad (3)$$

b – width

Equation 2 and Equation 3 can be manipulated to provide the thickness evolution as a function of time ($h_1(t)$); see Equation 4 for the plane-strain flow case.

$$h_1(t) = \sqrt{\left\{ \frac{2tW}{l\mu b^3} + \frac{1}{h_0^2} \right\}^{-1}} \quad (4)$$

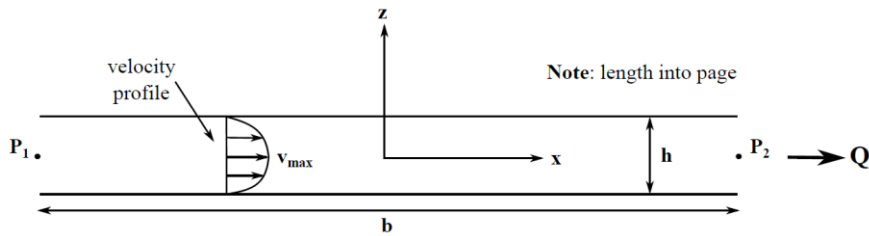


Figure 1: Flow Geometry

3 MATERIAL MODEL

Both Newtonian and non-Newtonian fluids were studied in this work. Rheology tests on the thermoplastics considered were conducted using a parallel disc, strain controlled rotation rheometer. Tests were conducted at four processing temperatures, between 165°C, 175°C, 185°C and 195°C. The viscosity vs. shear strain rate curves obtained are plotted in Figure 2, which indicate that the thermoplastic considered is a shear-thinning material [27].

To use the rigid-plastic solver in MSC/Marc, flow stress rather than viscosity of a material needs to be input. Considering pure shear that presents in the rheology tests, Equation 4 can be derived to relate the flow stress to viscosity, where σ_s , η and $\dot{\epsilon}$ are the flow stress, viscosity and effective strain rate respectively.

$$\sigma_s = 3\eta\dot{\epsilon} \quad (4)$$

In the present work, the relationship between the viscosity and shear rate as shown in Figure 2 was implemented into MSC/Marc using tabulated input. For shear rates below 0.0016 Hz¹ the viscosity is assumed to be constant, the Newtonian viscosities for each temperature can be seen in Table 2.

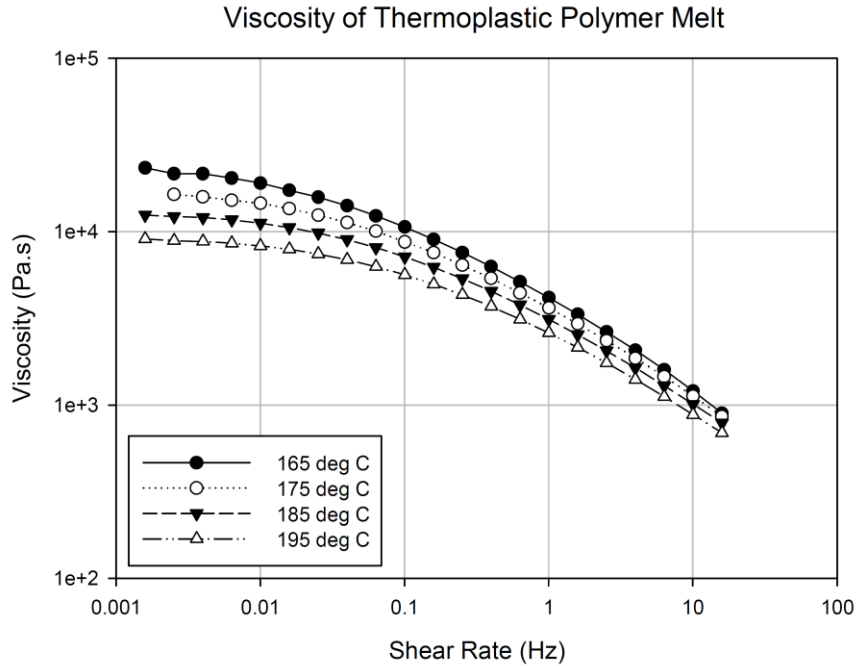


Figure 2: Viscosity of Thermoplastic Polymer Melt

4 FEA MODEL

4.1 Elements

The FEA analysis was conducted on MSC/Marc using its rigid-plastic solver. For the FEA of squeeze flows it is necessary to understand the elements that are being used and that they are capable of representing the material and boundary conditions that are present in the real world problem (necessary for both analytical and experimental validation). It was assumed that the polymer melt is incompressible and shows no elasticity after yield, and therefore is suitable to be modelled as rigid-plastic in which deformation is assumed to be plastic flow.

Three additional parameters are necessary for the analysis of rigid-plastic flow: 1) initial shear rate estimate, 2) shear rate cut-off, and 3) rigid-plastic incompressibility factor. The initial shear rate estimate is made using a Newtonian viscosity (in the constant region of <0.005Hz, Figure 2) and further manipulation of Equation 4 to produce an estimation for the velocity of the fluid between the platens (see Equation 6 and 7). The initial shear rate estimated can then be entered into the model parameters. The shear thinning behaviour is introduced as tabulated data in the material model as previously mentioned in Section 3.

¹ For 175°C, below a shear rate of 0.0025 Hz the viscosity is assumed to be constant.

$$V_{out} = \frac{V_c b}{2h_1} \quad (6)$$

$$shear\ rate = \frac{V_{out}}{h_1} \quad (7)$$

The element that has been chosen to model the squeeze flow between the two rigid platens is a quadrilateral, plain-strain, Herrmann formulation element which is suitable for modelling incompressible materials (Element 80) [28]. This element is also suitable for contact analyses and is capable of supporting the updated Lagrangian process which is necessary for modelling large strain problems. For cases in which parallel disc flow is to be modelled, a quadrilateral axisymmetric ring, Herrmann formulation element is suitable (Element 82) [28].

4.2 Geometry and boundary conditions

The geometries modelled in the simulations for this study are generally represented by Figure 3 in which the critical dimensions are the half width ($b/2$, where the full width of the joint is defined as b) and the initial thermoplastic thickness (h_0). The infinite length parallel plate cases can be analysed using half of the domain, as a line of symmetry exists halfway along the width (included in Figure 3); this reduces the computational time necessary to complete the simulation. The length of the bottom platen is not of concern, as long as the length is sufficient enough to contain the spew fillet.

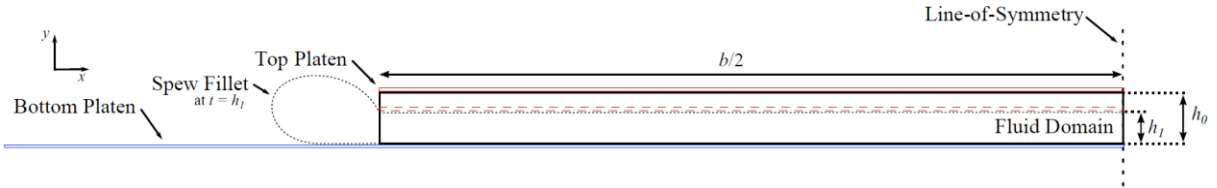


Figure 3: FEA Model Geometry – Infinite Length Parallel Plates

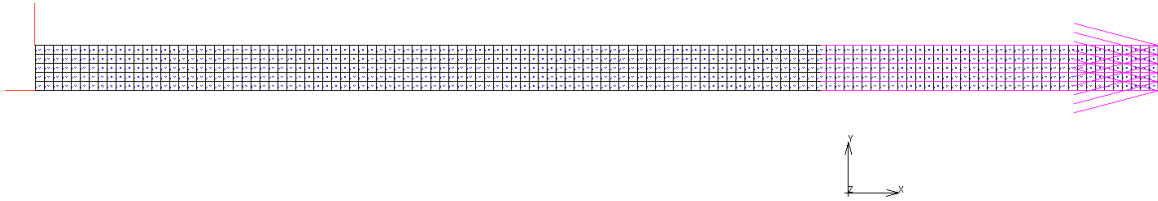


Figure 4: FEA Mesh Example ($h_0 = 250\mu\text{m}$, $b/2 = 6.25\text{mm}$)

For the model shown in Figure 3 four boundary conditions need to be implemented for the successful completion of the model. The four boundary conditions are: 1) load applied to the top platen (simulating a constant pressure), 2) symmetric boundary condition (at the line-of-symmetry), 3) fixed bottom platen, and 4) no-slip contact between the platens and the fluid domain. The first boundary condition was applied by specifying a force proportional to the width (b) of the plate and by fixing the top platen from rotating. The second boundary condition was applied by restricting the fluid domain nodes along the line-of-symmetry in the x -direction. The third boundary condition was applied by fixing the bottom platen from displacement and rotation. The fourth boundary condition was applied by specifying the contact between the platen and the fluid domain as glued (in MSC Mentat/MSC Marc). The correct application of these boundary conditions helps lead to a computationally efficient

finite element model [29].

Also, it should be noted that the elements used in these models were a consistent size for all models at $50\mu\text{m}$ square (see Figure 4). For example, an initial $h_0 = 250\mu\text{m}$ and $b/2 = 6.25\text{mm}$ gives a mesh density of 5 by 125 elements.

A parametric study was completed to study the effects of different widths (b) and welding temperatures; parameters modelled were: joint widths 12.5mm, 25mm, 35mm, 50mm, and 70mm; and temperatures 165°C , 175°C , 185°C , and 195°C . The aspect ratios (AR) were calculated using the width and initial thickness ($AR = b/h_0$, $h_0 = 250\mu\text{m}$) and shown in Table 1 (these aspect ratios are calculated using the width (b), not the half-width as seen in Figure 3). It is important to understand the aspect ratio (the platen width in comparison to the polymer thickness) to ensure that Assumption (iii) in Section 2 is satisfied. It was expected that the higher the aspect ratio, the smaller the error between the analytical solutions and FEA models. The analysis time was 900 seconds (or 15 minutes) for all models with a constant pressure of 100kPa.

Table 1: Aspect Ratio

Joint Width	12.5mm	25mm	35mm	50mm	70mm
AR	50	100	140	200	280

5 RESULTS AND DISCUSSION

The aim of this study was to build a framework in which the FEA models could be validated against solutions provided from analytical models. This section will present a summary of the results and provide a discussion on the important points. An example of the weld polymer flow for $h_1 = 250\mu\text{m}$, $b/2 = 6.25\text{mm}$, $t = 774.8$ seconds and a temperature of 165°C can be seen in Figure 5.

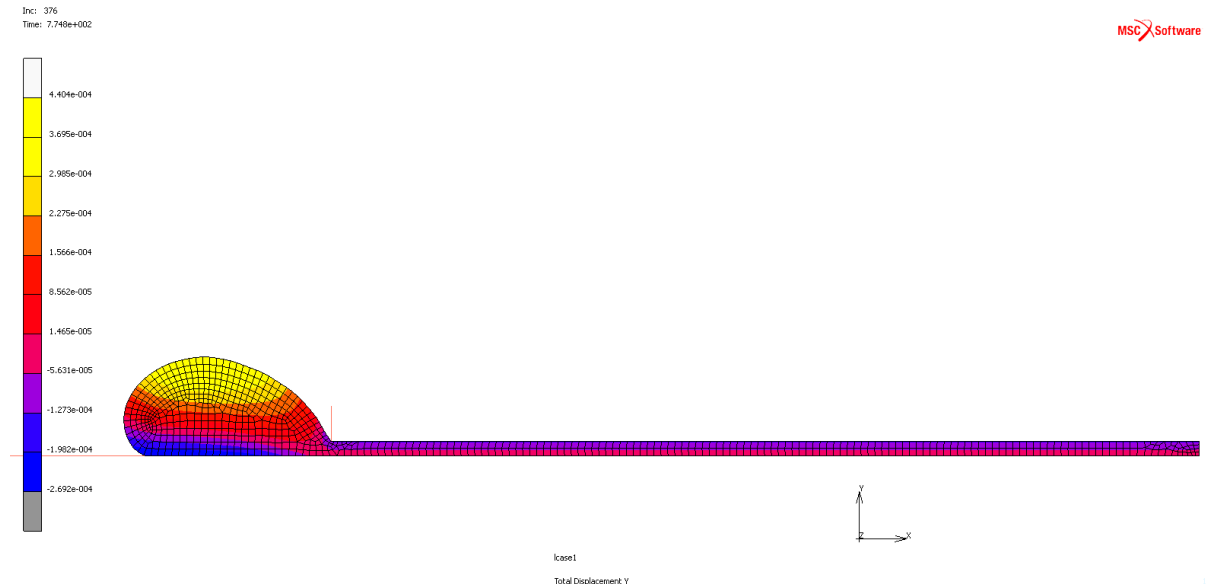


Figure 5: FEA Example of Squeeze Flow ($h_0 = 250\mu\text{m}$, $b/2 = 6.25\text{mm}$, $t = 774.8$ seconds, $T = 165^\circ\text{C}$), Total Displacement in Y Direction Shown

5.1 -Validation of FEA against Analytical Solution

The results of the analytical solutions provide an initial method of validation for the FEA models. Presented in Table 2 are the final thickness values calculated for each of the width and temperature combinations.

Table 2: Final Thickness in μm (from Analytical Models) for h_0 of $250\mu\text{m}$, Newtonian Viscosity

Temperature	Newtonian Viscosity	12.5mm	25mm	35mm	50mm	70mm
165	23389.3 Pa.s	123.8	187.9	211.8	228.9	238.6
175	16438.4 Pa.s	107.8	172.7	200.2	221.5	234.2
185	12467.8 Pa.s	96.0	159.9	189.7	214.3	229.7
195	9081.4 Pa.s	83.7	144.8	176.3	204.4	223.4

As has been mentioned in Section 2, analytical solutions can be used to calculate solutions for the final thickness of parallel discs (as well as this, FEA solutions can be presented for parallel discs). Table 3 shows the resulting thicknesses for a 17mm diameter parallel disc flow, with an initial thickness of $250\mu\text{m}$, under a force of 5N, for the four temperatures and viscosities shown in Table 2.

Table 3: Final Thickness in μm (from Analytical Models) for h_0 of $250\mu\text{m}$, Newtonian Viscosity, Parallel Discs

	165	175	185	195
Viscosity	23389.3 Pa.s	16438.4 Pa.s	12467.8 Pa.s	9081.4 Pa.s
Thickness	177.8	161.7	148.5	133.3

The FEA models built in MSC Mentat/MSC Marc with a Newtonian viscosity produced weld polymer thickness predictions comparable to those presented in Table 2. See Table 4.

Table 4: Final Thickness in μm (from FEA) for h_0 of $250\mu\text{m}$, Newtonian Fluid Material Model

Temperature	Newtonian Viscosity	12.5mm	25mm	35mm	50mm	70mm
165	23389.3 Pa.s	125.7	187.0	210.1	228.3	237.9
175	16438.4 Pa.s	110.5	171.5	199.0	220.5	233.8
185	12467.8 Pa.s	99.3	157.9	188.2	213.6	229.3
195	9081.4 Pa.s	86.4	143.7	174.0	204.0	221.8

As well as the FEA models produced for infinite length parallel plates, FEA models were built to model axisymmetric flow, using axisymmetric elements, for a comparison with Table 3, see Table 5.

Table 5: Final Thickness in μm (from FEA) for h_0 of $250\mu\text{m}$, Newtonian Fluid Material Model, Parallel Discs

	165	175	185	195
Viscosity	23389.3 Pa.s	16438.4 Pa.s	12467.8 Pa.s	9081.4 Pa.s
Thickness	176.7	157.3	146.9	133.0

Comparing the final weld polymer thickness values recorded in Table 2 and Table 4 it can be seen that the results obtained are very similar: see Figure 6. The average difference between the analytical solutions and the FEA predictions is 1%, with a maximum difference of 3.47%. A general trend can be noticed that the greater the aspect ratio (see Table 1) the smaller the difference between the analytical and FEA predictions: see Figure 7. This is due to the assumption underlying the analytical solution for the squeeze flow of a viscous fluid, Assumption (iii), that the thickness of the squeeze film is small compared with the plate dimensions. An exact aspect ratio above this assumption is reasonable is not provided; however, it seems as if an aspect ratio of 100 or greater provides a difference consistently less than 1%. Therefore, it can be said that the FEA simulation framework has been validated.

As well as the infinite length parallel plate situation analysed through analytical and FEA models, a parallel disc case has also been presented (see Table 3 and Table 5). The difference between the final polymer thicknesses for the analytical and FEA models for the parallel disc case was calculated as being approximately 1% (similar to that for the infinite length parallel plates). Therefore, for cases in which axisymmetric models are required to be simulated, the FEA framework is capable of producing accurate results.

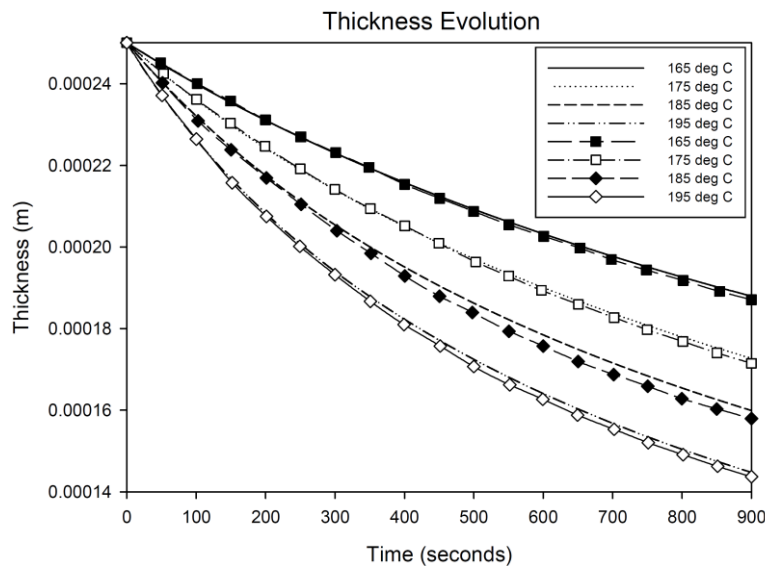


Figure 6: Analytical v. FEA (denoted by symbols) Thickness Evolution ($t = 900\text{sec}$, $b = 25\text{mm}$, $h_0 = 250\mu\text{m}$), Newtonian Viscosity

It can also be seen (for the infinite length parallel plate case) that the lower the viscosity, the greater the difference between the analytical and FEA predictions. This may be due to higher inertial effects accompanying the higher flow velocity of the material out of the joint.

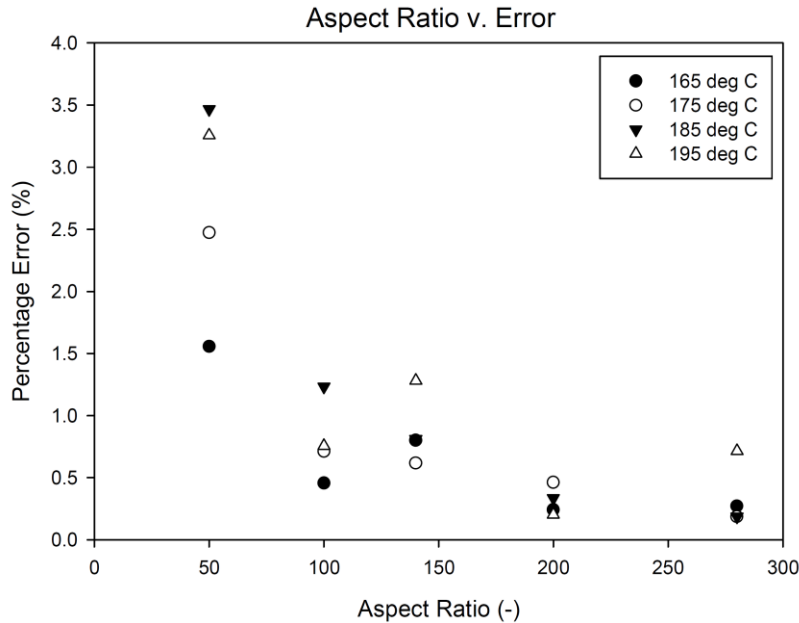


Figure 7 : Percentage Error between Analytical and FEA Solutions

5.2 Effect of non-Newtonian material model

A non-Newtonian fluid model was also implemented. The final thickness with a non-Newtonian fluid is less than that predicted for a Newtonian fluid.

Table 6: Final Thickness in μm (from FEA) for h_0 of $250\mu\text{m}$, non-Newtonian Fluid model

Temperature	12.5mm	25mm	35mm	50mm	70mm
165	101.2	162.6	194.0	220.8	235.3
175	88.5	149.8	181.7	212.5	230.3
185	79.3	137.8	169.7	204.2	223.5
195	69.9	125.1	156.4	191.9	214.8

The final thickness predicted for the parallel disc case, using a non-Newtonian (shear-thinning) viscosity, can be seen in Table 7.

Table 7: Final Thickness in μm (from FEA) for h_0 of $250\mu\text{m}$, non-Newtonian Fluid model, Parallel Discs

	165	175	185	195
Thickness	161.1	159.1	135.6	122.5

It can be seen in Figure 8 (and by comparing Table 4 and Table 6, and Table 5 and Table 7) that there is a significant difference between the final thicknesses predicted in the FEA simulations in which a non-Newtonian model has been implemented.

By analysing Figure 8, it can be seen that, for all temperatures, the non-Newtonian fluid model leads to significant difference in the predicted final thickness. This is due to the shear-thinning nature of the non-Newtonian fluid model. The non-Newtonian model predicts a smaller final thickness because for strain rates higher than 0.0016 Hz , the viscosity is lower

than the Newtonian fluid model, leading to greater flow. For example, in the 12.5mm wide fluid domain there is an average (across the four temperatures) 20% difference between the final thickness predicted by Newtonian and non-Newtonian models; for the 70mm wide fluid domain the average difference in the predictions is 2%. This is because the shear rates are much higher using the 12.5mm wide platen, due to the lower aspect ratio.

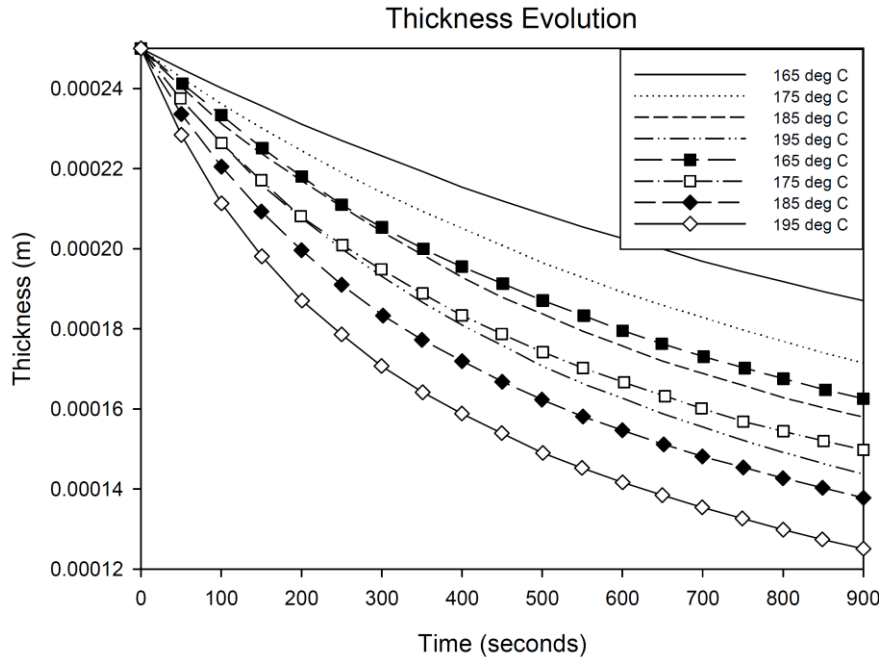


Figure 8 : FEA Thickness Evolution – Newtonian Viscosity v. non-Newtonian Viscosity (denoted by symbols), ($t = 900\text{sec}$, $b = 25\text{mm}$, $h_0 = 250\mu\text{m}$)

6 CONCLUSIONS & FUTURE WORK

It can be seen through the approach presented in this paper that finite element analysis methods are capable of representing squeeze flow between infinite length parallel plates and parallel discs. Validation against analytical solutions has been completed using Newtonian representations of the polymer melt. The shear-thinning behaviour of the thermoplastic polymer melt has been successfully modelled in MSC Mentat/MSC Marc. A solid framework has been developed which can be used for more complex investigations of squeeze flow.

In future work, the framework developed will be built upon, to be able to simulate cases which are not easily represented using analytical models. These models will include variations in temperature through the fluid domain, and complex platen geometries (including non-parallel, concave and convex platens, etc.) Models in which the top platen is an elastic body allowing for deformation will also be developed. This will help in the understanding of more realistic welding processes.

REFERENCES

- [1] M. J. Adams, İ. Aydin, B. J. Briscoe, and S. K. Sinha, "A finite element analysis of the squeeze flow of an elasto-viscoplastic paste material," *Journal of Non-Newtonian Fluid Mechanics*, vol. 71, pp. 41-57, 1997.
- [2] J. Engmann, C. Servais, and A. S. Burbidge, "Squeeze flow theory and applications to rheometry: A review," *Journal of Non-Newtonian Fluid Mechanics*, vol. 132, pp. 1-27, 2005.
- [3] D. F. Moore, "A review of squeeze films," *Wear*, vol. 8, pp. 245-263, 7// 1965.
- [4] O. Reynolds, "On the Theory of Lubrication and Its Application to Mr. Beauchamp Tower's Experiments, Including an Experimental Determination of the Viscosity of Olive Oil," *Philosophical Transactions of the Royal Society of London*, vol. 177, pp. 157-234, January 1, 1886 1886.
- [5] D. D. Fuller, *Theory and Practice of Lubrication for Engineers*. United States of America: John Wiley & Sons, Inc., 1956.
- [6] A. J. Smiley, M. Chao, and J. W. Gillespie Jr, "Influence and control of bondline thickness in fusion bonded joints of thermoplastic composites," *Composites Manufacturing*, vol. 2, pp. 223-232, 1991.
- [7] D. F. Hays, "Squeeze Films for Rectangular Plates," *Journal of Basic Engineering*, vol. 85, pp. 243-246, 1963.
- [8] J. D. Sherwood, "Squeeze flow of a power-law fluid between non-parallel plates," *Journal of Non-Newtonian Fluid Mechanics*, vol. 166, pp. 289-296, 2011.
- [9] B. Hoffner, O. H. Campanella, M. G. Corradini, and M. Peleg, "Squeezing flow of a highly viscous incompressible liquid pressed between slightly inclined lubricated wide plates," *Rheologica Acta*, vol. 40, pp. 289-295, 2001/05/01 2001.
- [10] B. t. Debbaut, "Non-isothermal and viscoelastic effects in the squeeze flow between infinite plates," *Journal of Non-Newtonian Fluid Mechanics*, vol. 98, pp. 15-31, 2001.
- [11] A. N. Alexandrou, G. C. Florides, and G. C. Georgiou, "Squeeze flow of semi-solid slurries," *Journal of Non-Newtonian Fluid Mechanics*, vol. 193, pp. 103-115, 2013.
- [12] G. C. Florides, A. N. Alexandrou, and G. C. Georgiou, "Flow development in compression of a finite amount of a Bingham plastic," *Journal of Non-Newtonian Fluid Mechanics*, vol. 143, pp. 38-47, 2007.
- [13] G. Karapetsas and J. Tsamopoulos, "Transient squeeze flow of viscoplastic materials," *Journal of Non-Newtonian Fluid Mechanics*, vol. 133, pp. 35-56, 2006.
- [14] A. Lawal and D. M. Kalyon, "Compressive squeeze flow of generalized Newtonian fluids with apparent wall slip," *INTERNATIONAL POLYMER PROCESSING*, vol. 15, pp. 63-71, 2000.
- [15] N. Phan-thien, F. Sugeng, and R. I. Tanner, "The squeeze-film flow of a viscoelastic fluid," *Journal of Non-Newtonian Fluid Mechanics*, vol. 24, pp. 97-119, 1987.
- [16] D. M. Kalyon and H. S. Tang, "Inverse problem solution of squeeze flow for parameters of generalized Newtonian fluid and wall slip," *Journal of Non-Newtonian Fluid Mechanics*, vol. 143, pp. 133-140, 2007.
- [17] D. T. Gethin, R. W. Lewis, and M. R. Tadayan, "A FINITE-ELEMENT APPROACH FOR MODELING METAL FLOW AND PRESSURIZED SOLIDIFICATION IN THE SQUEEZE CASTING PROCESS," *International Journal for Numerical Methods in*

- Engineering*, vol. 35, pp. 939-950, 1992.
- [18] R. W. Lewis, E. W. Postek, Z. Han, and D. T. Gethin, "A finite element model of the squeeze casting process," *International Journal of Numerical Methods for Heat & Fluid Flow*, vol. 16, pp. 539-572, 2006.
- [19] R. W. Lewis, Z. Q. Han, and D. T. Gethin, "Three-dimensional finite element model for metal displacement and heat transfer in squeeze casting processes," *Comptes Rendus Mécanique*, vol. 335, pp. 287-294, 2007.
- [20] G. Winther, K. Almdal, and O. Kramer, "Determination of polymer melt viscosity by squeezing flow with constant plate velocity," *Journal of Non-Newtonian Fluid Mechanics*, vol. 39, pp. 119-136, // 1991.
- [21] G. Brindley, J. M. Davies, and K. Walters, "Elastico-viscous squeeze films. part I," *Journal of Non-Newtonian Fluid Mechanics*, vol. 1, pp. 19-37, 1976.
- [22] E. A. MOSS, A. KRASSNOKUTSKI, B. W. SKEWS, and R. T. PATON, "Highly transient squeeze-film flows," *Journal of Fluid Mechanics*, vol. 671, pp. 384-398, 2011.
- [23] A. P. Jackson, X.-L. Liu, and R. Paton, "Squeeze flow characterisation of thermoplastic polymer," *Composite Structures*, vol. 75, pp. 179-184, 9// 2006.
- [24] P. J. Leider, "Squeezing Flow between Parallel Disks. II. Experimental Results," *Industrial & Engineering Chemistry Fundamentals*, vol. 13, pp. 342-346, 1974/11/01 1974.
- [25] Y. Deng, G. C. Martin, G. P. Kohut, and J. T. Gotro, "The rheological characterization of fluorinated thermoplastics using squeezing flow viscometry," *Polymer Engineering and Science*, vol. 34, pp. 213-213, 1994.
- [26] P. Shirodkar and S. Middleman, "Lubrication Flows in Viscoelastic Liquids. I. Squeezing Flow between Approaching Parallel Rigid Planes," *Journal of Rheology*, vol. 26, pp. 1-17, 1982.
- [27] N. P. Cheremisinoff, *Encyclopedia of fluid mechanics* vol. 7. Houston U6 - ctx_ver=Z39.88-2004&ctx_enc=info%3Aofi%2Fenc%3AUTF-8&rft_id=info:sid/summon.serialssolutions.com&rft_val_fmt=info:ofi/fmt:kev:mtx:book&rft.genre=book&rft.title=Encyclopedia+of+fluid+mechanics&rft.au=Cheremisinoff%2C+Nicholas+P&rft.date=1985-01-01&rft.pub=Gulf+Pub.+Co.%2C+Book+Division&rft.externalDBID=n%2Fa&rft.externalDocID=b1192536x¶mdict=en-US U7 - Book U8 - FETCH-uq_catalog_b1192536x1: Gulf Pub. Co., Book Division, 1985.
- [28] (2013, Marc 2013 - Volume B: Element Library. [User's Manual]. 11, 431-434, 440-443.
- [29] G. Liu and S. Quek, *The finite element method: a practical course*. Oxford: Butterworth Heinemann, 2003.